Journal of Solid Mechanics Vol. 8, No. 1 (2016) pp. 31-44

Closed Form Solution for Electro-Magneto-Thermo-Elastic Behaviour of Double-Layered Composite Cylinder

A. Loghman *, H. Parsa

Department of Solid Mechanics, Faculty of Mechanical Engineering, University of Kashan, Islamic Republic of Iran

Received 2 September 2015; accepted 8 December 2015

ABSTRACT

Electro-magneto-thermo-elastic response of a thick double-layered cylinder made from a homogeneous interlayer and a functionally graded piezoelectric material (FGPM) outer layer is investigated. Material properties of the FGPM layer vary along radius based on the power law distribution. The vessel is subjected to an internal pressure, an induced electric potential, a uniform magnetic field and a temperature gradient. Stresses and radial displacement are studied for different material in-homogeneity parameters β in the FGPM layer. It has been shown that the material in-homogeneity parameters β significantly affect the stress distribution in both layers. Therefore by selecting a suitable material parameter β one can control stress distribution in both homogeneous and FGPM layers. It has been found that under electro-magneto-thermo-mechanical loading minimum effective stress can be achieved by selecting $\beta = -1.5$ in the FGPM layer.

Keywords : Closed form solution; Electromagnetothermoelastic; Double-walled cylinder; Homogeneous interlayer; FGPM outer layer.

1 INTRODUCTION

MATERIAL tailoring and analysis of components to withstand the combined thermal, mechanical and dynamical loadings have been attracted many researchers attention in the past two decades [1]. Analysis of single block cylinders made of functionally graded piezoelectric material has been considered by many investigators. Babaei and Chen [2] presented an analytical solution for the electromechanical response of a rotating functionally graded piezoelectric hollow cylinder. A piezoelectric hollow cylinder with thermal gradient has been investigated by Saadatfar and Razavi [3]. Ghorbanpour et al. [4] studied the effect of material inhomogeneity parameter on electro-thermo-mechanical response of functionally graded piezoelectric rotating shafts. Electrothermomechanical behavior of a radially polarized rotating functionally graded piezoelectric cylinder has been considered by Ghorbanpour et al. [5]. Analysis of Multi-walled cylinders with different materials has also been an active area of research in recent years [6]. Mithchell and Reddy [7] have studied an embedded piezoelectric layer in composite cylinders. Dynamic response of a multilayered orthotropic piezoelectric hollow cylinder for axisymmetric plane strain condition has been presented by Wang and Chen [8]. Transient plane-strain responses of multilayered elastic cylinders to axisymmetric impulse have been considered by Yin and Yue [9]. Magnetothermoelastic interactions in hollow structures of functionally graded material subjected to mechanical loads have been considered by Dai and Fu [10]. Dynamic thermoelastic behavior of a double-layered

*Corresponding author. Tel.: +98 31 55912425; Fax: +98 31 55912424.
E-mail address: aloghman@kashanu.ac.ir (A. Loghman).

hollow cylinder with an FGM layer has been presented by Dai and Rao [11]. An exact solution for magneto-thermo-elastic behaviour of double-walled cylinder made of an inner FGM and an outer homogeneous layer has been presented by Loghman and Parsa [12].

The main objective of this paper is to obtain a closed form solution for electro-magneto-thermo-elastic response of double-walled cylinder made of an inner homogeneous layer and an outer FGPM layer.

2 GEOMETRY AND LOADING CONDITION

A thick double-walled hollow long cylinder with an inner radius a_1, an interface radius of a_2 and outer radius a_3 is considered. The interlayer is homogeneous and the outer layer is made from FGPM material. The FGPM material's property varies along radius based on the power law distribution. The material in both homogeneous and FGPM layers are assumed to be independent of temperature. Loading is composed of internal pressure P_i, external pressure P_o, a uniform magnetic field in axial direction and a temperature field due to steady state heat conduction. The FGPM layer is also subjected to an electric potential difference. It is assumed that no separation will occur longitudinally or radially for all loading combinations. Geometry and loading combination is shown in Fig. 1.

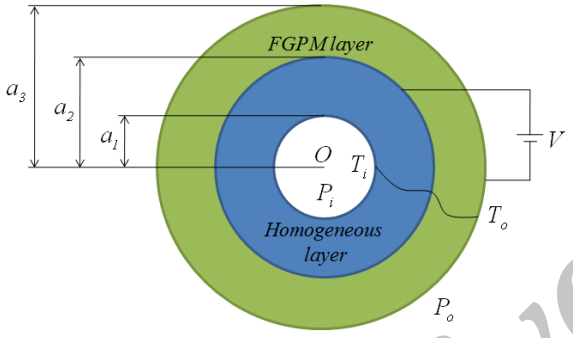

Fig.1
Geometry and loading condition of double-walled long cylinder made of an inner homogeneous and an outer FGPM layer.

3 HEAT CONDUCTION FORMULATION

Heat conduction equation in the cylindrical coordinate system with the thermal boundary condition (T1 in the inner radius and T3 in the outer radius) is given as [13]:

$$\frac{1}{r}\frac{\partial}{\partial r}\left[rk(r)\frac{\partial T(r)}{\partial r}\right]=0 \tag{1}$$

k_h and $k_p = k_{0p}r^{\beta}$ are the thermal conduction coefficients of the homogeneous and FGPM layers in hollow cylinder in radial direction. Substituting these coefficients into the heat conduction Eq. (1) the general solution for the temperature distribution is obtained as:

$$T_h(r) = M_{1h}\ln r + M_{2h} \qquad a_1 \le r \le a_2 \qquad for\ \text{homogeneous}\ layer \tag{2}$$

$$T_p(r) = M_{1p}r^{-\beta} + M_{2p} \qquad a_2 \le r \le a_3 \qquad for\ FGPM\ layer \tag{3}$$

where the subscripts *h* and *p* are for homogeneous and piezoelectric layers. The thermal boundary conditions for the double-walled hollow long cylinder are:

$$\begin{cases} 1: T_h(a_1) = T_1 \Rightarrow M_{1h} \ln a_1 + M_{2h} = T_1 \\ 2: T_p(a_3) = T_3 \Rightarrow M_{1p} a_3^{-\beta} + M_{2p} = T_3 \\ 3: T_h(a_2) = T_p(a_2) \Rightarrow M_{1h} \ln a_2 + M_{2h} = M_{1p} a_2^{-\beta} + M_{2p} \\ 4: q_h(a_2) = q_p(a_2) \Rightarrow -k_h A_h \dfrac{\partial T_h}{\partial r}(a_2) = -k_p A_p \dfrac{\partial T_p}{\partial r}(a_2) \end{cases} \tag{4}$$

where M_{1h} and M_{2h} and M_{1p} and M_{2p} are obtained from the thermal boundary conditions as follows:

$$M_{1h} = \frac{T_3 - T_1}{(\ln a_2 - \ln a_1) - \dfrac{k_h}{k_{0p}\beta}(a_3^{-\beta} - a_2^{-\beta})} \quad , M_{2h} = T_1 - \ln a_1 \; M_{1h} \tag{5}$$

$$M_{1p} = -\frac{k_h}{k_{0p}\beta} \frac{T_3 - T_1}{(\ln a_2 - \ln a_1) - \dfrac{k_h}{k_{0p}\beta}(a_3^{-\beta} - a_2^{-\beta})}, \; M_{2p} = T_3 - a_3^{-\beta} M_{1p} \tag{6}$$

Substituting M_{1h}, M_{2h}, M_{1p} and M_{2p} into Eqs . (2) and (3) the temperature distribution in homogeneous and FGPM layers are obtained for different values of β and shown in Fig. 2.

4 ELECTRO-MAGNETO-THERMO-ELASTIC FORMULATION

Radial, circumferential and axial stresses in the homogeneous layer under axisymmetric geometry and loading condition can be written in terms of displacement as follows:

$$\begin{cases} \sigma_{rh} = \bar{c}_{11} \dfrac{\partial u}{\partial r} + \bar{c}_{12} \dfrac{u}{r} - \bar{\lambda}_1 T(r) \\ \sigma_{\theta h} = \bar{c}_{12} \dfrac{\partial u}{\partial r} + \bar{c}_{22} \dfrac{u}{r} - \bar{\lambda}_2 T(r) \\ \sigma_{zh} = \bar{c}_{13} \dfrac{\partial u}{\partial r} + \bar{c}_{23} \dfrac{u}{r} - \bar{\lambda}_3 T(r) \end{cases} \tag{7}$$

The subscript *h* is for the homogeneous layer . The coefficients in the above equation are written as:

$$\bar{c}_{11} = \bar{c}_{22} = \frac{E(1-\nu)}{(1+\nu)(1-2\nu)}, \; \bar{c}_{12} = \bar{c}_{13} = \bar{c}_{23} = \frac{E\nu}{(1+\nu)(1-2\nu)}, \; \bar{\lambda}_i = \bar{c}_{ij} \; \bar{\alpha}_j \tag{8}$$

The equation of equilibrium for the homogeneous layer in the presence of magnetic field in axial direction is written as follows

$$\frac{\partial \sigma_{rh}}{\partial r} + \frac{\sigma_{rh} - \sigma_{\theta h}}{r} + f(r) = 0 \tag{9}$$

In which $f(r)$ is the Lorentz's force written as follows [9]:

$$f(r) = \mu(r) H_z^2 \frac{\partial}{\partial r}\left(\frac{\partial u}{\partial r} + \frac{u}{r}\right) \tag{10}$$

Substituting Eq. (7) and Eq. (8) and Eq. (10) into Eq. (9) , Eq. (11) is obtained as follows:

$$(\bar{c}_{11}+\mu_0 H_z^2)\frac{\partial^2 u}{\partial r^2}+(\bar{c}_{11}+\mu_0 H_z^2)\frac{\partial u}{\partial r}r^{-1}+(-\bar{c}_{22}-\mu_0 H_z^2)ur^{-2}=\bar{\lambda}_1\frac{\partial T(r)}{\partial r}+(\bar{\lambda}_1-\bar{\lambda}_2)T(r)r^{-1} \tag{11}$$

Eq. (11) can be rewritten as follows:

$$\frac{\partial^2 u}{\partial r^2}+\bar{I}_1 r^{-1}\frac{\partial u}{\partial r}+\bar{I}_2 r^{-2}u=\bar{I}_3\frac{\partial T(r)}{\partial r}+\bar{I}_4 T(r)r^{-1} \tag{12}$$

where ccoefficients in Eq. (12) are written as:

$$\bar{I}_1=\frac{\bar{c}_{11}+\mu_0 H_z^2}{\bar{c}_{11}+\mu_0 H_z^2}=1\ ,\quad \bar{I}_2=\frac{-\bar{c}_{22}-\mu_0 H_z^2}{\bar{c}_{11}+\mu_0 H_z^2}\ ,\quad \bar{I}_3=\frac{\bar{\lambda}_1}{\bar{c}_{11}+\mu_0 H_z^2}\ ,\quad \bar{I}_4=\frac{\bar{\lambda}_1-\bar{\lambda}_2}{\bar{c}_{11}+\mu_0 H_z^2} \tag{13}$$

Stress-strain relations in the FGPM layer under axisymmetric geometry and loading condition in terms of radial displacement, electric potential and temperature field are given as [14,15]

$$\begin{cases}\sigma_{rp}=c_{11}(r)\dfrac{\partial u}{\partial r}+c_{12}(r)\dfrac{u}{r}+e_{11}(r)\dfrac{\partial \psi}{\partial r}-\lambda_1 T(r)\\ \sigma_{\theta p}=c_{12}(r)\dfrac{\partial u}{\partial r}+c_{22}(r)\dfrac{u}{r}+e_{12}(r)\dfrac{\partial \psi}{\partial r}-\lambda_2 T(r)\\ \sigma_{zp}=c_{13}(r)\dfrac{\partial u}{\partial r}+c_{23}(r)\dfrac{u}{r}+e_{13}(r)\dfrac{\partial \psi}{\partial r}-\lambda_3 T(r)\end{cases} \tag{14}$$

The subscript p is for the FGPM layer. Electrostatic charge equation in the FGPM layer may be written as:

$$D_r=e_{11}\frac{\partial u}{\partial r}+e_{12}\frac{u}{r}-g_1\frac{\partial \psi}{\partial r}+p_1 T(r) \tag{15}$$

Coefficients in Eq. (14) and Eq. (15) are written as:

$$\begin{aligned}&c_{ij}=c_{0ij}r^{\beta}\ ,\quad e_{1j}=e_{01j}r^{\beta}\ ,\quad \alpha_j=\alpha_{0j}r^{\beta}\ ,\quad \mu(r)=\mu_0 r^{\beta}\ ,\quad g_1=g_{01}r^{\beta}\ ,\quad p_1=p_{01}r^{\beta}\ ,\\ &\lambda_i=c_{ij}\,\alpha_j=c_{0ij}\alpha_{0j}r^{2\beta}=\lambda_{0i}r^{2\beta}\end{aligned} \tag{16}$$

Equation of equilibrium for the FGPM layer in the presence of magnetic field in axial direction is written as follows

$$\frac{\partial \sigma_{rp}}{\partial r}+\frac{\sigma_{rp}-\sigma_{\theta p}}{r}+f(r)=0 \tag{17}$$

The charge equation of electrostatics in the absence of free charge density, is given as [15]

$$\frac{\partial D_r}{\partial r}+\frac{D_r}{r}=0 \tag{18}$$

By solving the Eq. (18) the electrical displacement is obtained as:

$$D_r=\frac{A_1}{r} \tag{19}$$

Substituting Eq. (19) into Eq. (15) , Eq. (20) is obtained as follows

$$\frac{\partial \psi}{\partial r} = (e_{11}\frac{\partial u}{\partial r} + e_{12}\frac{u}{r} + p_1 T(r) - \frac{A_1}{r}) / g_1 \tag{20}$$

Substituting Eq. (20) into Eq. (14) and then using equilibrium Eq. (17) the following differential equation for the FGPM layer is obtained

$$\frac{\partial^2 u}{\partial r^2} + I_1 \frac{\partial u}{\partial r} r^{-1} + I_2 u r^{-2} = I_3 \frac{\partial T(r)}{\partial r} + I_4 \frac{\partial T(r)}{\partial r} r^{\beta} + I_5 T(r) r^{-1} + I_6 T(r) r^{\beta-1} + I_7 A_1 r^{-2-\beta} \tag{21}$$

Coefficients in Eq. (21) are written as:

$$\begin{aligned}
&I_1 = (c_{011} + \frac{e_{011}^2}{g_{01}} + \mu_0 H_z^2)^{-1} \cdot ((\beta+1)(c_{011} + \frac{e_{011}^2}{g_{01}}) + \mu_0 H_z^2) \\
&I_2 = (c_{011} + \frac{e_{011}^2}{g_{01}} + \mu_0 H_z^2)^{-1} \cdot ((\beta-1)(c_{012} + \frac{e_{011} e_{012}}{g_{01}}) - \mu_0 H_z^2 + c_{012} - c_{022} + \frac{e_{012}(e_{011} - e_{012})}{g_{01}}) \\
&I_3 = -\frac{e_{011} p_{01}}{g_{01}} (c_{011} + \frac{e_{011}^2}{g_{01}} + \mu_0 H_z^2)^{-1} \qquad I_4 = \lambda_{01} (c_{011} + \frac{e_{011}^2}{g_{01}} + \mu_0 H_z^2)^{-1} \\
&I_5 = (c_{011} + \frac{e_{011}^2}{g_{01}} + \mu_0 H_z^2)^{-1} \cdot (\frac{e_{012} p_{01}}{g_{01}} - (\beta+1)\frac{e_{011} p_{01}}{g_{01}}) \\
&I_6 = (c_{011} + \frac{e_{011}^2}{g_{01}} + \mu_0 H_z^2)^{-1} \cdot ((2\beta+1)\lambda_{01} - \lambda_{02}) \qquad I_7 = -(c_{011} + \frac{e_{011}^2}{g_{01}} + \mu_0 H_z^2)^{-1} \frac{e_{012}}{g_{01}}
\end{aligned} \tag{22}$$

Substituting $\frac{\partial T(r)}{\partial r}$ and $T(r)$ into Eq. (12) and Eq. (21) the following differential equations for homogeneous and FGPM layers are obtained as follows

$$\begin{aligned}
&\frac{\partial^2 u}{\partial r^2} + \bar{I}_1 r^{-1} \frac{\partial u}{\partial r} + \bar{I}_2 r^{-2} u = \bar{I}_5 r^{-1} + \bar{I}_6 r^{-1} \ln r \\
&\bar{I}_5 = \bar{I}_3 M_{1h} + \bar{I}_4 M_{2h} \qquad \bar{I}_6 = \bar{I}_4 M_{1h}
\end{aligned} \tag{23}$$

$$\begin{aligned}
&\frac{\partial^2 u}{\partial r^2} + I_1 r^{-1} \frac{\partial u}{\partial r} + I_2 r^{-2} u = I_8 r^{\beta-1} + I_9 r^{-1} + I_{10} r^{-\beta-1} + I_7 F_1 r^{-\beta-2} \\
&I_8 = I_6 M_{2p} \qquad I_9 = -I_4 \beta M_{1p} + I_5 M_{2p} + I_6 M_{1p} \qquad I_{10} = -I_3 \beta M_{1p} + I_5 M_{1p}
\end{aligned} \tag{24}$$

5 SOLUTION OF DIFFERENTIAL EQUATIONS

General solution of the above differential equations can be obtained by substituting $u = cr^m$ in Eqs. (23) and (24) leading to the following solution for the homogeneous and FGPM layers as:

$$\bar{u}_g = \bar{C}_1 r^{\bar{m}_1} + \bar{C}_2 r^{\bar{m}_2} \qquad \bar{m}_{1,2} = \frac{-(\bar{I}_1 - 1) \pm \sqrt{(\bar{I}_1 - 1)^2 - 4\bar{I}_2}}{2} \tag{25}$$

$$u_g = C_1 r^{m_1} + C_2 r^{m_2} \qquad m_{1,2} = \frac{-(I_1 - 1) \pm \sqrt{(I_1 - 1)^2 - 4I_2}}{2} \tag{26}$$

Particular solution of differential Eqs. (23) and (24) can be written as follows

$$\begin{aligned} &\bar{u}_p = \bar{C}_3 r \ln r + \bar{C}_4 r \\ &\bar{C}_3 = \frac{\bar{I}_6}{\bar{I}_1 + \bar{I}_2} \qquad \bar{C}_4 = \frac{\bar{I}_5(\bar{I}_1 + \bar{I}_2) - \bar{I}_6(\bar{I}_1 + 1)}{(\bar{I}_1 + \bar{I}_2)^2} \end{aligned} \tag{27}$$

$$\begin{aligned} &u_P = C_3 r^{\beta+1} + C_4 r + C_5 r^{-\beta+1} + C_6 F_1 r^{-\beta} \\ &C_3 = \frac{I_8}{(\beta+1)\beta + I_1(\beta+1) + I_2} \quad C_4 = \frac{I_9}{I_1 + I_2} \\ &C_5 = \frac{I_{10}}{(\beta-1)\beta + I_1(1-\beta) + I_2} \quad C_6 = \frac{I_7}{(\beta+1)\beta - I_1\beta + I_2} \end{aligned} \tag{28}$$

And finally the solution for homogeneous and FGPM layer is obtained as:

$$\bar{u}_{\text{homogeneous}} = \bar{u}_g + \bar{u}_p = \bar{C}_1 r^{\bar{m}_1} + \bar{C}_2 r^{\bar{m}_2} + \bar{C}_3 r \ln r + \bar{C}_4 r \tag{29}$$

$$u_{FGPM} = u_g + u_p = C_1 r^{m_1} + C_2 r^{m_2} + C_3 r^{\beta+1} + C_4 r + C_5 r^{-\beta+1} + C_6 A_1 r^{-\beta} \tag{30}$$

Substituting Eq.(30) into Eq.(20) , yields

$$\begin{aligned} &\frac{\partial \psi}{\partial r} = C_1 \left(\frac{m_1 e_{011} + e_{012}}{g_{01}}\right) r^{m_1 - 1} + C_2 \left(\frac{m_2 e_{011} + e_{012}}{g_{01}}\right) r^{m_2 - 1} + C_3 \left(\frac{(\beta+1) e_{011} + e_{012}}{g_{01}}\right) r^{\beta} \\ &+ C_4 \left(\frac{e_{011} + e_{012}}{g_{01}}\right) + \frac{p_{01} M_{2p}}{g_{01}} + \frac{C_5 \left[(1-\beta) e_{011} + e_{012}\right] + p_{01} M_{1p}}{g_{01}} r^{-\beta} + \left(\frac{C_6(-\beta e_{011} + e_{012}) - 1}{g_{01}}\right) A_1 r^{-\beta-1} \end{aligned} \tag{31}$$

with integrating Eq. (31) , electric potential distribution is obtained as:

$$\begin{aligned} &\psi(r) = C_1 \left(\frac{m_1 e_{011} + e_{012}}{m_1 g_{01}}\right) r^{m_1} + C_2 \left(\frac{m_2 e_{011} + e_{012}}{m_2 g_{01}}\right) r^{m_2} + C_3 \left(\frac{(\beta+1) e_{011} + e_{012}}{(\beta+1) g_{01}}\right) r^{\beta+1} \\ &+ \left[C_4 \left(\frac{e_{011} + e_{012}}{g_{01}}\right) + \frac{p_{01} M_{2p}}{g_{01}} \right] r + \frac{C_5 \left[(1-\beta) e_{011} + e_{012}\right] + p_{01} M_{1p}}{(-\beta+1) g_{01}} r^{-\beta+1} + \\ &\left(\frac{C_6(\beta e_{011} - e_{012}) + 1}{\beta g_{01}}\right) A_1 r^{-\beta} + A_2 \end{aligned} \tag{32}$$

The solution for radial, circumferential and axial stresses in homogeneous layer are obtained with substituting Eqs. (29) and (5) into Eq. (7) as follows

$$\begin{cases} \sigma_{rh} = \bar{C}_1 \bar{Q}_{11} r^{\bar{m}_1 - 1} + \bar{C}_2 \bar{Q}_{12} r^{\bar{m}_2 - 1} + \bar{Q}_{13} lnr + \bar{Q}_{14} \\ \sigma_{\theta h} = \bar{C}_1 \bar{Q}_{21} r^{\bar{m}_1 - 1} + \bar{C}_2 \bar{Q}_{22} r^{\bar{m}_2 - 1} + \bar{Q}_{23} lnr + \bar{Q}_{24} \\ \sigma_{zh} = \bar{C}_1 \bar{Q}_{31} r^{\bar{m}_1 - 1} + \bar{C}_2 \bar{Q}_{32} r^{\bar{m}_2 - 1} + \bar{Q}_{33} lnr + \bar{Q}_{34} \end{cases} \tag{33}$$

The solution for radial, circumferential and axial stresses in FGPM layer are obtained with substituting Eqs. (30), (31) and (6) into Eq. (14) as follows

$$\begin{cases}\sigma_{rp}=C_1Q_{11}r^{\beta+m_1-1}+C_2Q_{12}r^{\beta+m_2-1}+Q_{13}r^{2\beta}+Q_{14}r^{\beta}+Q_{15}+Q_{16}A_1r^{-1}\\ \sigma_{\theta p}=C_1Q_{21}r^{\beta+m_1-1}+C_2Q_{22}r^{\beta+m_2-1}+Q_{23}r^{2\beta}+Q_{24}r^{\beta}+Q_{25}+Q_{26}A_1r^{-1}\\ \sigma_{zp}=C_1Q_{31}r^{\beta+m_1-1}+C_2Q_{32}r^{\beta+m_2-1}+Q_{33}r^{2\beta}+Q_{34}r^{\beta}+Q_{35}+Q_{36}A_1r^{-1}\end{cases} \tag{34}$$

Coefficients of Eqs. (33) and (34) are written in appendix A. Considering an internal pressure of P_i and an external pressure of P_0 and the potential electric in a_2 and potential electric in a_3 and continuity of radial stress and displacement at the interface of two layers the following boundary conditions must be satisfied

$$\begin{cases}1:\sigma_r(a_1)=-P_i \Rightarrow \bar{x}_1(a_1)\bar{C}_1+\bar{y}_1(a_1)\bar{C}_2+\bar{z}_1(a_1)=-P_i\\ 2:\sigma_{rh}(a_2)=\sigma_{rp}(a_2)\Rightarrow \bar{x}_1(a_2)\bar{C}_1+\bar{y}_1(a_2)\bar{C}_2+\bar{z}_1(a_2)=x_1(a_2)C_1\\ \qquad\qquad +y_1(a_2)C_2+z_1(a_2)+z_2(a_2)A_1\\ 3:u_{rh}(a_2)=u_{rp}(a_2)\Rightarrow \bar{x}_2(a_2)\bar{C}_1+\bar{y}_2(a_2)\bar{C}_2+\bar{z}_2(a_2)=x_2(a_2)C_1\\ \qquad\qquad +y_2(a_2)C_2+z_3(a_2)+z_4(a_2)A_1\\ 4:\sigma_{rp}(a_3)=-P_o \Rightarrow x_1(a_3)C_1+y_1(a_3)C_2+z_1(a_3)+z_2(a_3)A_1=-P_o\\ 5:\psi(a_2)=\psi_{a_2}\Rightarrow B_1(a_2)C_1+B_2(a_2)C_2+E(a_2)A_1+F(a_2)+A_2=\psi_{a_2}\\ 6:\psi(a_3)=\psi_{a_3}\Rightarrow B_1(a_3)C_1+B_2(a_3)C_2+E(a_3)A_1+F(a_3)+A_2=\psi_{a_3}\end{cases} \tag{35}$$

Coefficients in Eq. (35) are written in appendix B. With solution of boundary conditions unknown parameters are obtained as:

$$\begin{aligned}&A_1=W_1C_1+W_2C_2+W_3\\ &A_2=\psi_{a_3}-B_1(a_3)C_1-B_2(a_3)C_2-F(a_3)-E(a_3)(A_1)\\ &\bar{C}_1=\frac{O_2K_2-L_2K_1}{L_1O_2-L_2O_1}\qquad \bar{C}_2=-\frac{P_i+\bar{z}_1(a_1)}{\bar{y}_1(a_1)}-\frac{\bar{x}_1(a_1)}{\bar{y}_1(a_1)}\left(\frac{O_2K_2-L_2K_1}{L_1O_2-L_2O_1}\right)\\ &C_1=\frac{O_1K_2-L_1K_1}{L_1O_2-L_2O_1}\qquad C_2=-\frac{P_o+Z_1(a_3)}{Y_1(a_3)}-\frac{X_1(a_3)}{Y_1(a_3)}\left(\frac{O_1K_2-L_1K_1}{L_1O_2-L_2O_1}\right)\end{aligned} \tag{36}$$

The coefficients in the Eq. (36) are written in appendix C.

5 RESULTS AND DISCUSSION

The results presented in this paper are based on the data written in the Tables 1. and 2 for material properties ,geometry and loading condition for the inner homogeneous and outer FGPM layer.

Table 1
Material properties.

	$\bar{c}_{11}(GPa)$	$\bar{c}_{12}(GPa)$	$\bar{c}_{22}(GPa)$	$\bar{c}_{13}(GPa)$	$\bar{c}_{23}(GPa)$
Homogeneous material	312.7	134	312.7	134	134
	$\bar{\alpha}(K^{-1})$	$\bar{\mu}_0(Hm^{-1})$	$k_h(Wm^{-1}K^{-1})$		
	5.87×10^{-6}	$4\pi\times10^{-7}$	13.723		
	$c_{011}(GPa)$	$c_{012}(GPa)$	$c_{022}(GPa)$	$c_{013}(GPa)$	$c_{023}(GPa)$
FGPM material	111	77.8	220	115	115
	$\alpha_{01}(K^{-1})$	$\alpha_{02}(K^{-1})$	$\alpha_{03}(K^{-1})$	$\mu_0(Hm^{-1})$	$k_{0P}(Wm^{-1}K^{-1})$
	10×10^{-5}	1×10^{-5}	10×10^{-5}	$4\pi\times10^{-7}$	1.5
	$e_{011}(Cm^{-2})$	$e_{012}(Cm^{-2})$	$e_{013}(Cm^{-2})$	$g_{01}(C^2m^{-2}N^{-1})$	$p_{01}(C^2m^{-2}K^{-1})$
	15.1	-5.2	-5.2	5.62×10^{-9}	-2.5×10^{-5}

Table 2
Geometry and loading condition.

	$l(m)$	$\psi(KWA^{-1})$	$P(MPa)$	$T(K)$	$Hz\ (Am^{-1})$
a_1	1	----------	100	30	2.23×10^9 (uniform)
a_2	1.5	0	----------	----------	
a_3	2	100	0	0	

Temperature distribution due to steady state heat conduction for different values of β is shown in Fig. 2. It is obvious from this figure that the temperature gradient in the homogeneous layer is much lower than the FGPM layer which is justified by its higher heat conduction coefficient written in Table 1. Electric potential distribution just occurs in the FGPM layer because of its piezoelectric material property. Electric potential distribution due to an external imposed electric potential for different values of β is shown in Fig. 3. Electric potential distribution will occur in the FGPM layer for any distinct or loading combination. Distribution of the induced electric potential due to internal pressure and temperature field are shown for various β in Fig. 4 and 5. In both figures the electric boundary conditions are satisfied and the negative or positive values of electric potential can be justified by their respective radial displacements shown in Figs. 6 and 7. As we can see in the FGPM layer of Fig. 6 the radial strain ($\varepsilon_r = \frac{du}{dr}$) which is the slope of the radial displacement is negative while in Fig. 7 in the FGPM layer radial strain is positive. Radial stresses due to internal pressure, applied electric potential, electro-thermo-mechanical and electro-magneto-thermo-mechanical loading combination is shown in Figs. 8, 9, 10 and 11. All radial stresses satisfy the continuity condition at the interface and the boundary conditions at the inner and outer surfaces of the double layered vessel. Significant effect of magnetic field on radial stresses can be observed by comparing Figs. 10 and 11. Circumferential stresses of internal pressure, electric potential, electro-thermo-mechanical and electro-magneto-thermo-mechanical loading combinations are shown in Figs. 12, 13, 14 and 15. Fig. 12 indicates that the circumferential stresses of internal pressure in the homogeneous layer is indeed the classical Lame tangential stresses however in the FGPM layer higher values of circumferential stresses belong to higher absolute values of radial stresses at the interface which can be considered as an internal pressure for the outer layer. Thermoelastic circumferential stresses in the homogeneous layer are not significant as shown in Fig. 13. This is because of small temperature gradient in this layer. In the FGPM layer thermo-elastic circumferential stresses are compressive at the inner region and are tensile at the outer region of the vessel. This is because in the presence of high temperature gradient the outer layers are at lower temperatures than the inner layers and therefore they will be stretched by the high temperature layers while the inner layers will be left in compression as is clear in Fig. 13. Circumferential stresses of combined internal pressure, thermal gradient and an imposed electric potential are shown in Fig. 14. In this case electrothermoelastic stresses are nearly the sum of elastic and thermoelastic stresses shown in Figs. 12 and 13. This is because mechanical and thermal stresses are dominant due to high internal pressure and thermal gradient while the imposed electric potential is not really considerable. Magnetic field has a significant effect on circumferential stresses as can be observed by comparing Figs. 15 and 14. Effective electrothermoelastic and electromagnetithermoelastic Von Mises stresses are shown in Figs. 16 and 17. Under electro-magneto-thermo-mechanical loading combination minimum effective stress distribution can be achieved by selecting $\beta = -1.5$ in the FGPM layer.

The results reported in this paper are for a few selected combination of mechanical, thermal, electro-thermo-mechanical and electro-magneto-thermo-mechanical loadings and material grading index. However the closed form solution presented in this paper can be used for any combination of loading and material properties.

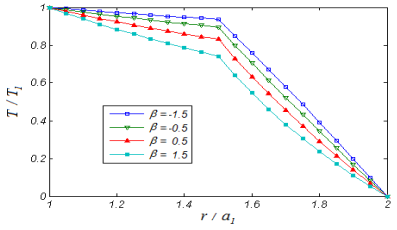

Fig.2
Temperature field due to steady state heat conduction for various β .

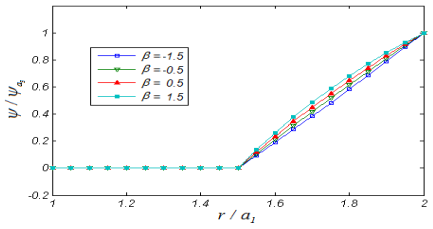

Fig.3
Electric potential distribution due to an imposed potential difference on the FGPM layer for various β .

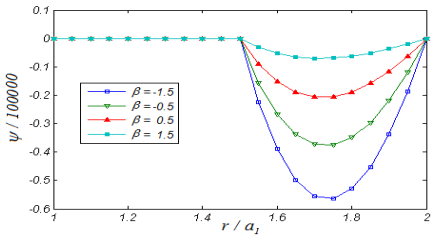

Fig.4
Electric potential distribution due to internal pressure for various β .

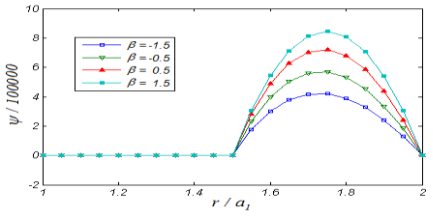

Fig.5
Electric potential distribution due to temperature field for various β .

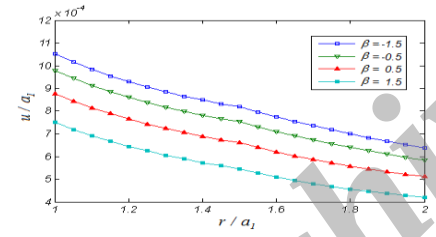

Fig.6
Radial displacement due to internal pressure for various β .

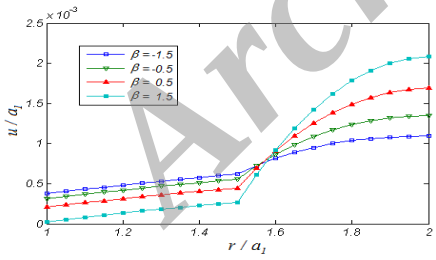

Fig.7
Radial displacement due to temperature field for various β .

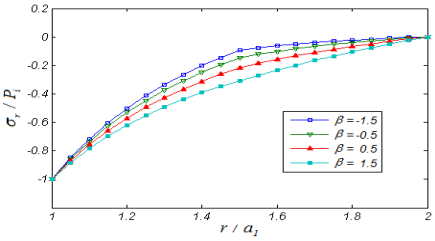

Fig.8
Elastic radial stresses due to internal pressure for various β .

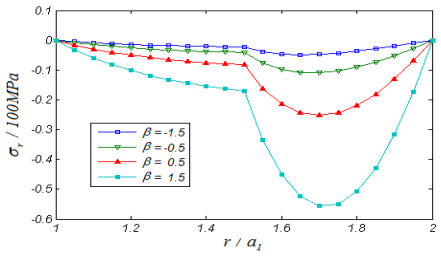

Fig.9
Thermoelastic radial stresses due to temperature field for various β .

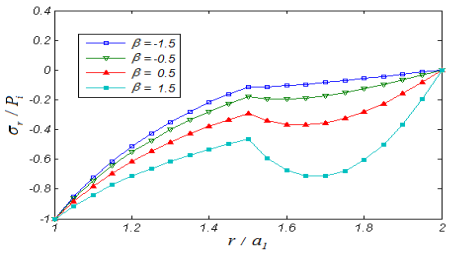

Fig.10
Electrothermoelastic radial stresses for various β .

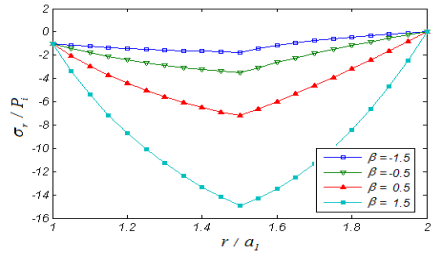

Fig.11
Electromagnetothermoelastic radial stresses for various β .

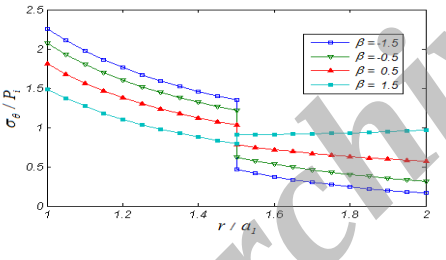

Fig.12
Elastic circumferential stresses due to internal pressure for various β .

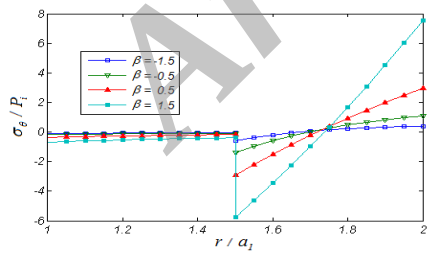

Fig.13
Thermoelastic circumferential stresses due to temperature field for various β .

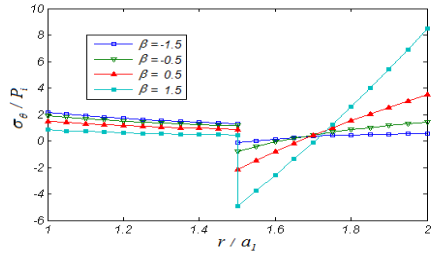

Fig.14
Electrothermoelastic circumferential stresses for various β .

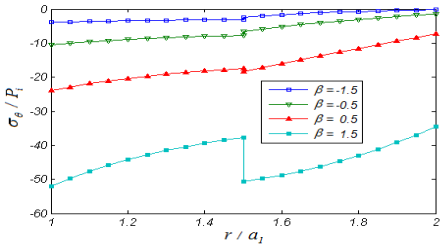

Fig.15
Electromagnetothermoelastic circumferential stresses for various β .

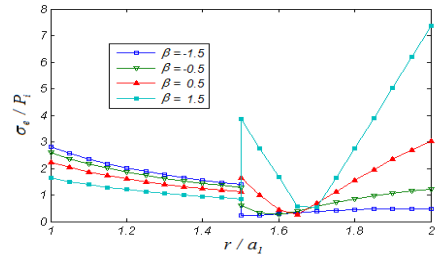

Fig.16
Electrothermoelastic effective Von Mises stresses for various β .

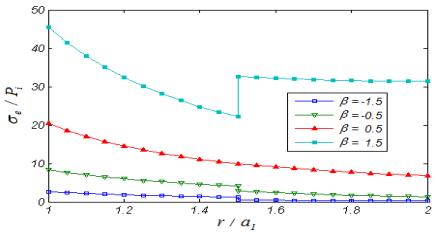

Fig.17
Electromagnetothermoelastic effective Von Mises stresses for various β .

7 CONCLUSIONS

A double-walled cylinder made of an inner homogeneous and an outer FGPM layer under electro-magneto-thermo-mechanical loading is studied. The closed form solution presented for stresses and displacements in both homogeneous and FGPM layers can be used for any combination of electrical, mechanical, magnetic and thermal loading. Stress distribution in the homogeneous and FGPM layers depends on the material in-homogeneity parameter β . Therefore by selecting a suitable material parameter β in the FGPM layer one can control stress distribution in both homogeneous and FGPM layers. It has been found that under electro-magneto-thermo-mechanical loading combination minimum effective stress distribution can be achieved by selecting $\beta = -1.5$ in the FGPM layer.

APPENDIX A

The coefficients in the Eq. (33) are defined as follows:

$$\bar{Q}_{11} = \bar{m}_1\bar{c}_{11} + \bar{c}_{12} \quad \bar{Q}_{12} = \bar{m}_2\bar{c}_{11} + \bar{c}_{12} \quad \bar{Q}_{13} = \bar{C}_3(\bar{c}_{11} + \bar{c}_{12}) - \bar{\lambda}_1 M_{1h} \quad \bar{Q}_{14} = \bar{C}_4(\bar{c}_{11} + \bar{c}_{12}) + \bar{C}_3\bar{c}_{11} - \bar{\lambda}_1 M_{2h}$$
$$\bar{Q}_{21} = \bar{m}_1\bar{c}_{12} + \bar{c}_{22} \quad \bar{Q}_{22} = \bar{m}_2\bar{c}_{12} + \bar{c}_{22} \quad \bar{Q}_{23} = \bar{C}_3(\bar{c}_{12} + \bar{c}_{22}) - \bar{\lambda}_2 M_{1h} \quad \bar{Q}_{24} = \bar{C}_4(\bar{c}_{12} + \bar{c}_{22}) + \bar{C}_3\bar{c}_{12} - \bar{\lambda}_2 M_{2h}$$
$$\bar{Q}_{31} = \bar{m}_1\bar{c}_{13} + \bar{c}_{23} \quad \bar{Q}_{32} = \bar{m}_2\bar{c}_{13} + \bar{c}_{23} \quad \bar{Q}_{33} = \bar{C}_3(\bar{c}_{13} + \bar{c}_{23}) - \bar{\lambda}_3 M_{1h} \quad \bar{Q}_{34} = \bar{C}_4(\bar{c}_{13} + \bar{c}_{23}) + \bar{C}_3\bar{c}_{13} - \bar{\lambda}_3 M_{2h}$$

And the coefficients in the Eq. (34) are written as:

$$Q_{11}=m_1c_{011}+c_{012}+e_{011}\frac{m_1e_{011}+e_{012}}{g_{01}} \qquad Q_{12}=m_2c_{011}+c_{012}+e_{011}\frac{m_2e_{011}+e_{012}}{g_{01}}$$

$$Q_{13}=C_3((\beta+1)c_{011}+c_{012}+e_{011}\frac{(\beta+1)e_{011}+e_{012}}{g_{01}})-\lambda_{01}M_{2p}$$

$$Q_{14}=C_4(c_{011}+c_{012}+e_{011}\frac{e_{011}+e_{012}}{g_{01}})+e_{011}\frac{p_{01}M_{2p}}{g_{01}}-\lambda_{01}M_{1p}$$

$$Q_{15}=C_5((-\beta+1)c_{011}+c_{012}+e_{011}\frac{(1-\beta)e_{011}+e_{012}}{g_{01}}))+e_{011}\frac{p_{01}M_{1p}}{g_{01}}$$

$$Q_{16}=C_6(-\beta c_{011}+c_{012}+e_{011}\frac{-\beta e_{011}+e_{012}}{g_{01}})-\frac{e_{011}}{g_{01}}$$

$$Q_{21}=m_1c_{012}+c_{022}+e_{012}\frac{m_1e_{011}+e_{012}}{g_{01}} \qquad Q_{22}=m_2c_{012}+c_{022}+e_{012}\frac{m_2e_{011}+e_{012}}{g_{01}}$$

$$Q_{23}=C_3((\beta+1)c_{012}+c_{022}+e_{012}\frac{(\beta+1)e_{011}+e_{012}}{g_{01}})-\lambda_{02}M_{2p}$$

$$Q_{24}=C_4(c_{012}+c_{022}+e_{012}\frac{e_{011}+e_{012}}{g_{01}})+e_{012}\frac{p_{01}M_{2p}}{g_{01}}-\lambda_{02}M_{1p}$$

$$Q_{25}=C_5((-\beta+1)c_{012}+c_{022}+e_{012}\frac{(1-\beta)e_{011}+e_{012}}{g_{01}}))+e_{012}\frac{p_{01}M_{1p}}{g_{01}}$$

$$Q_{26}=C_6(-\beta c_{012}+c_{022}+e_{012}\frac{-\beta e_{011}+e_{012}}{g_{01}})-\frac{e_{012}}{g_{01}}$$

$$Q_{31}=m_1c_{013}+c_{023}+e_{013}\frac{m_1e_{011}+e_{012}}{g_{01}} \qquad Q_{32}=m_2c_{013}+c_{023}+e_{013}\frac{m_2e_{011}+e_{012}}{g_{01}}$$

$$Q_{33}=C_3((\beta+1)c_{013}+c_{023}+e_{013}\frac{(\beta+1)e_{011}+e_{012}}{g_{01}})-\lambda_{03}M_{2p}$$

$$Q_{34}=C_4(c_{013}+c_{023}+e_{013}\frac{e_{011}+e_{012}}{g_{01}})+e_{013}\frac{p_{01}M_{2p}}{g_{01}}-\lambda_{03}M_{1p}$$

$$Q_{35}=C_5((-\beta+1)c_{013}+c_{023}+e_{013}\frac{(1-\beta)e_{011}+e_{012}}{g_{01}}))+e_{013}\frac{p_{01}M_{1p}}{g_{01}}$$

$$Q_{36}=C_6(-\beta c_{013}+c_{023}+e_{013}\frac{-\beta e_{011}+e_{012}}{g_{01}})-\frac{e_{013}}{g_{01}}$$

APPENDIX B

The coefficients in the Eq. (35) are defined as follows:

$$\bar{x}_1(r)=\bar{Q}_{11}r^{\bar{m}_1-1} \qquad \bar{y}_1(r)=\bar{Q}_{12}r^{\bar{m}_2-1} \qquad \bar{z}_1(r)=\bar{Q}_{13}\ln r+\bar{Q}_{14}$$

$$\bar{x}_2(r)=r^{\bar{m}_1} \qquad \bar{y}_2(r)=r^{\bar{m}_2} \qquad \bar{z}_2(r)=\bar{C}_3 r\ln r+\bar{C}_4 r$$

$$x_1(r)=Q_{11}r^{\beta+m_1-1} \qquad y_1(r)=Q_{12}r^{\beta+m_2-1} \qquad z_1(r)=Q_{13}r^{2\beta}+Q_{14}r^{\beta}+Q_{15}$$

$$x_2(r)=r^{m_1} \qquad y_2(r)=r^{m_2} \qquad z_2(r)=Q_{16}r^{-1}$$

$$z_3(r)=C_3r^{\beta+1}+C_4r+C_5r^{-\beta+1} \qquad z_4(r)=C_6r^{-\beta}$$

$$B_1(r)=(\frac{m_1e_{011}+e_{012}}{m_1g_{01}})r^{m_1} \qquad B_2(r)=(\frac{m_2e_{011}+e_{012}}{m_2g_{01}})r^{m_2} \qquad E(r)=(\frac{C_6(\beta e_{011}-e_{012})+1}{\beta g_{01}})r^{-\beta}$$

$$F(r)=C_3(\frac{(\beta+1)e_{011}+e_{012}}{(\beta+1)g_{01}})r^{\beta+1}+\left[C_4(\frac{e_{011}+e_{012}}{g_{01}})+\frac{p_{01}M_{2p}}{\bar{g}_{01}}\right]r+\frac{C_5\left[(1-\beta)e_{011}+e_{012}\right]+p_{01}M_{1p}}{(-\beta+1)g_{01}}r^{-\beta+1}$$

APPENDIX C

The coefficients in the Eq. (36) are written as**:**

$$W_1=\frac{B_1(a_2)-B_1(a_3)}{E(a_3)-E(a_2)} \qquad W_2=\frac{B_2(a_2)-B_2(a_3)}{E(a_3)-E(a_2)} \qquad W_3=\frac{\psi_{a_3}-\psi_{a_2}-(F(a_3)-F(a_2))}{E(a_3)-E(a_2)}$$

$$X_1(r)=x_1(r)+z_2(r)N_1 \qquad X_2(r)=x_2(r)+z_4(r)N_1$$

$$Y_1(r)=y_1(r)+z_2(r)N_2 \qquad Y_2(r)=y_2(r)+z_4(r)N_2$$

$$Z_1(r)=z_1(r)+z_2(r)N_3 \qquad Z_2(r)=z_3(r)+z_4(r)N_3$$

$$L_1=\bar{x}_2(a_2)-\frac{\bar{x}_1(a_1)}{\bar{y}_1(a_1)}\bar{y}_2(a_2) \qquad L_2=X_2(a_2)-\frac{X_1(a_3)}{Y_1(a_3)}Y_2(a_2)$$

$$O_1=\bar{x}_1(a_2)-\frac{\bar{y}_1(a_2)}{\bar{y}_1(a_1)}\bar{x}_1(a_1) \qquad O_2=X_1(a_2)-\frac{Y_1(a_2)}{Y_1(a_3)}X_1(a_3)$$

$$K_1=\frac{\bar{y}_1(a_2)}{\bar{y}_1(a_1)}(P_i+\bar{z}_1(a_1))-\frac{Y_1(a_2)}{Y_1(a_3)}(P_o+Z_1(a_3))-\bar{z}_1(a_2)+Z_1(a_2)$$

$$K_2=\frac{\bar{y}_2(a_2)}{\bar{y}_1(a_1)}(P_i+\bar{z}_1(a_1))-\frac{Y_2(a_2)}{Y_1(a_3)}(P_o+Z_1(a_3))-\bar{z}_2(a_2)+Z_2(a_2)$$

ACKNOWLEDGEMENT

The authors are grateful to University of Kashan for financial supporting of this research work.

REFERENCES

[1] Nie G.J., Batra R.C., 2010, Material tailoring and analysis of functionally graded isotropic and incompressible linear elastic hollow cylinders, *Composite Structures* **92**: 265-274.

[2] Babaei M.H., Chen Z.T., 2008, Analytical solution for the electromechanical behaviour of a rotating functionally graded piezoelectric hollow cylinder, *Archive of Applied Mechanics* **78**: 489-500.

[3] Saadatfar M., Razavi A.S., 2009, Piezoelectric hollow cylinder with thermal gradient, *Journal of Mechanical Science and Technology* **23**: 45-53.

[4] Ghorbanpour Arani A., Kolahchi R., Mosallaie Barzoki A.A., 2010, Effect of material inhomogeneity on electro-thermo-mechanical behaviors of functionally graded piezoelectric rotating shaft, *Applied Mathematical Modelling* **36**: 2771-2789.

[5] Ghorbanpour Arani A., Loghman A., Abdollahitaheri A., Atabakhshian V., 2010, Electrothermomechanical behavior of a radially polarized rotating functionally graded piezoelectric cylinder, *Journal of Mechanics of Materials and Structures* **6**(6): 869-884.

[6] Haghpanah Jahromi B., Ajdari A., Nayeb-Hashemi H., Vaziri A., 2010, Autofrettage of layered and functionally graded metal–ceramic composite vessels, *Composite Structures* **92**(8): 1813-1822.

[7] Mithchell J.A., Reddy J.N., 1995, A study of embedded piezoelectric layers in composite cylinders, *Journal of Applied Mechanics* **62**:166-173.

[8] Wang H.M., Ding H.J., Chen Y.M., 2005, Dynamic solution of a multilayered orthotropic piezoelectric hollow cylinder for axisymmetric plane strain problems, *International Journal of Solids and Structures* **42**:85-102.

[9] Yin X.C., Yue Z.Q., 2002, Transient plane-strain response of multilayered elastic cylinders to axisymmetric impulse, *Journal of Applied Mechanics* **69**: 825-835.

[10] Dai H.L., Fu Y.M., 2007, Magnetothermoelastic interactions in hollow structures of functionally graded material subjected to mechanical loads, *International Journal of Pressure Vessels and Piping* **84**(3): 132-138.

[11] Dai H.L., Rao Y.N., 2013, Dynamic thermoelastic behavior of a double-layered hollow cylinder with an FGM layer, *Journal of Thermal Stresses* **36**(9): 962-984.

[12] Loghman A., Parsa H., 2014, Exact solution for magneto-thermo-elastic behaviour of double-walled cylinder made of an inner FGM and an outer homogeneous layer, *International Journal of Mechanical Sciences* **88**: 93-99.

[13] Hosseini S.M., Akhlaghi M., Shakeri M., 2007, Transient heat conduction in functionally graded thick hollow cylinders by analytical method, *International Journal of Heat and Mass Transfer* **43**: 669-675.

[14] Loghman A., Ghorbanpour Arani A., Amir S., Vajedi S., 2010, Magnetothermoelastic creep analysis of functionally graded cylinders, *International Journal of Pressure Vessel and Piping* **87**: 389-395.

[15] Dai H.L., Hong L., Fu Y.M., Xiao X., 2010, Analytical solution for electromagnetothermoelastic behaviors of a functionally graded piezoelectric hollow cylinder, *Applied Mathematical Modelling* **34**(2): 343-357.